IOP Conference Series: Materials Science and Engineering

PAPER • **OPEN ACCESS**

Microstructure and wear behaviour of high alloyed hot-work tool steels 1.2343 and 1.2367 under thermo-mechanical loading

To cite this article: I Y Malik *et al* 2019 *IOP Conf. Ser.: Mater. Sci. Eng.* **629** 012011

IOP Conf. Series: Materials Science and Engineering **629** (2019) 012011 doi:10.1088/1757-899X/629/1/012011

Microstructure and wear behaviour of high alloyed hot-work tool steels 1.2343 and 1.2367 under thermo-mechanical loading

I Y Malik[1,2], U Lorenz[1], A Chugreev[1] and B-A Behrens[1]

Institute of Forming Technology and Machines (IFUM) - Leibniz University Hannover, An der Universität 2, 30823 Garbsen, Germany

E-mail: malik@ifum.uni-hannover.de

Abstract. Tools and their maintenance costs in hot forging processes account for a considerable proportion of the total components' costs. Forging tools undergo extreme heating and subsequent cooling during the forging process and between the forging cycles, respectively. This cyclic heating and cooling of the tool surfaces leads to local changes in the tool microstructure which result in hardening or softening of the material in different regions of the tool and consequently influence the tool strength. Temperature in the tool areas experiencing high thermo-mechanical loadings can exceed the austenitic temperature. Hence, a strong cooling, for example by spraying or lubrication, can lead to formation of a martensitic layer in the boundary zone of the tool. Due to its higher hardness, martensitic layer has greater resistance to wear as compared to the basic or tempered materials. In the scope of this paper, the austenitisation behaviours of two high alloyed hot-work tool steels, 1.2343 and 1.2367, have been characterized by means of dilatometer tests to obtain time-temperature-austenitisation (TTA) diagrams for specimen under thermo-mechanical loads. Moreover, continuous-cooling-transformation (CCT) diagrams were recorded. Metallographic investigations were carried out to gather a detailed understanding of the microstructure behaviour and its resulting hardness. With the results of this works, it is aimed to gather a detailed and accurate insight into the arising hardening and softening effects. This would eventually lead to an optimisation of the numerical modelling for tool wear prediction.

1. Introduction

Hot-working tool steels are generally employed as tool material in hot forging processes. The tools in these processes are exposed to high mechanical, thermal and tribological stresses which lead to various types of damage [1]. The mechanical and thermal crack formation, plastic deformation and tool surface wear are, in particular, the primary reasons of failure in hot forging tools [2]. The tool surface wear is mainly caused due to the loss of material hardness in the areas close to the surface. This hardness loss is because of thermal stress induced as a result of the large heat transfer from the workpiece to the tool surface during the contact [3]. Owing to the high pressure in the tool-workpiece contact area, in combination with high tribological stresses, the surface temperature of forging tools increases considerably [4]. The alternating forging operations and lubricant application lead to a cyclic heating and cooling of the tool surface during the process. This in return results in material annealing and to a softening of the material in the surface layer. However, there are certain die regions, like convex radiuses, where the surface temperatures exceed the material austenitisation temperature [5]. In combination with high cooling rates, martensitic structures with a high hardness are generated in these regions. Both, softening as well as hardening of the tool material have a great influence on the wear resistance of the

forging tools [6]. Thus, the knowledge about the service life and reliability as well as the associated efficiency of the forging tools is of great importance [7].

Due to the above mentioned loadings, the forging tools undergo rapid temperature changes during forming processes as well as during heat treatment operations [8]. The temperature-time profile experienced by the tools during hot forging processes significantly influences their behaviour. As the material diffusion is a time-dependent variable, the heating or cooling rate has a considerable influence on the crystalline state of the metallic material. Different representations which take into account the time dependency of the transformations are considered during heating and cooling of the considered steel tools. During the heating, time-temperature-austenitisation diagram (TTA) is chosen which describes the microstructural transformations as well as the initial microstructure including grain growth. TTA diagrams are prepared in order to show achievable austenitisation states with as little grain growth as possible with several heating rates (θ_h). On the contrary, during cooling the behaviour of the microstructure is represented by means of continuous-cooling-transformation (CCT) and time-temperature-transformation (TTT) diagrams. For a CCT diagram, the specimen is continuously cooled after austenitisation to room temperature at various cooling rates ($\theta_{c)}$. Whereas, for the TTT diagram, the specimen is quenched to a desired testing temperature and then held until all transformations have taken place [9]. These diagrams are either provided by steel manufacturers or listed in heat treatment databanks [10, 11]. Nonetheless, the experimental process boundary conditions have a great influence on these diagrams. Thus, Behrens et al. in an earlier work have suggested using transformation diagrams for the process conditions being considered [12]. This paper describes the austenitisation behaviour (TTA) under influence of thermo-mechanical loads as well as the continuous cooling transformation (CCT) behaviour at various cooling rates for two high alloyed hot-work tool steels.

2. Material and specimen production method

In the scope of this work, two high alloyed hot-work tool steels 1.2343 (X37CrMoV5-1) and 1.2367 (X38CrMoV5-3) have been analysed. The chemical composition for both of these steels was measured by optical emission spectroscopy. The content of main alloying elements for both the steels is listed in table 1. Both consist of high chromium content. Other alloying elements are manganese, molybdenum, silicon and vanadium.

Table 1. Chemical composition of the tool steels under consideration (wt. %).

	C	Si	Mn	Cr	Mo	V
1.2343	0.41	0.97	0.32	4.77	1.30	0.46
1.2367	0.42	0.28	0.37	4.90	2.95	0.52

In order to obtain a homogenous cooling inside the specimen, hollow cylindrical specimen with length 10 mm, inner diameter 3.2 mm and outer diameter of 4 mm, i.e. 0.4 mm wall thickness (S_0) are used for the investigation performed in this work (figure. 1, a). The production of these thin-walled hollow specimens poses a major challenge. The manufacturing process of the hollow specimen must ensure that the initial structure is not influenced during specimen production and that the specimen faces are plane-parallel to each other. For this purpose, holes of diameter 3.2 mm were drilled into plates with a thickness of 10 mm and subsequently the plates are heat treated to a hardness of 45 HRC (450 HV0.2) by vacuum hardening. The hollow specimens were then separated from the hardened plates using the erosion by wire method. Due to the precise positioning of the wire, very small cutting widths as well as sharp-edged holes can be achieved with this method, which are also characterized by a very low heat-affected zone.

3. Experimental investigation

In order to carry out the experiments, the quenching and forming dilatometer DIL 805 A/D+T (manufacturer: TA Instruments) available at the IFUM was used. During the tests, a temperature measurement of the specimen is necessary to evaluate the thermal loads that actually occur. For this

purpose, type S thermocouples from Bähr Thermoanalyse GmbH with a wire thickness of 0.1 mm were welded onto the outer surface of the hollow specimens to measure and regulate the temperature. The connection of specimen and thermocouple was made by spot welding. During spot welding, the joint is flooded with gas to prevent oxidation or corrosion of the joint. With this method, a measuring range from 0 °C to 1700 °C with a measuring accuracy of 0.5 °C at the specimen surface can be measured. The change in length (ΔL) of the specimen due to heating and phase transformation is measured continuously via the push rods. Figure 1 shows the quenching (b) as well as deformation test (c) setup inside the dilatometer.

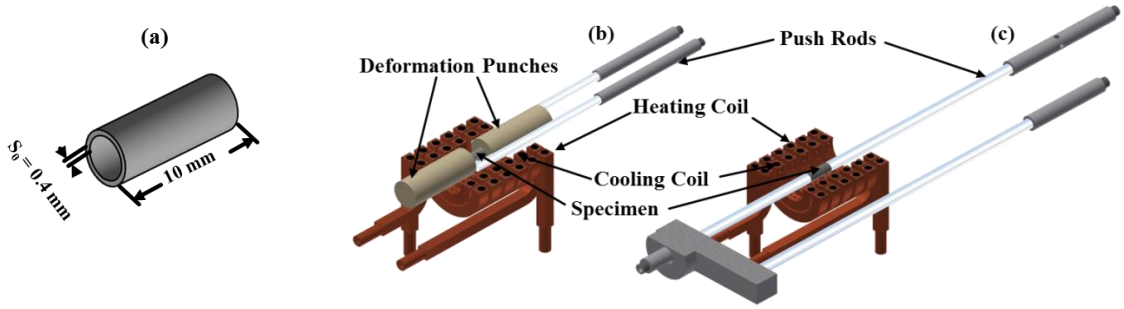

Figure 1. Schematic diagram of the hollow specimen (a); deformation module (b) and quenching module (c) of the quenching and forming dilatometer.

3.1. Time-temperature-austenitisation (TTA) diagram

The deformation and forming module of the dilatometer was used for characterizing the austenisation behaviour of the tool steels. As a result of the phase transformation, the specimen volume changes. For steel materials, austenitisation is characterised by the transformation of the lattice from body-centred cubic (bcc) into the surface-centred cubic (fcc) microstructure. With a constant temperature increase, an approximately linear increase in the change in length is observed until the transformation range is reached. This is characterised by a decrease in volume of the sample length despite a further increase in temperature and indicates the bcc to fcc lattice transformation. The temperature at the beginning of the phase transformation corresponds to the austenite start temperature (Ac_1), the temperature at complete austenitisation is called the austenite end temperature (Ac_3). An intermediate state exists between Ac_1 and Ac_3 whereas the Ac_3 indicates that the entire microstructure has converted to austenite. The Ac_1 or Ac_3 temperatures can be determined from the change in length - temperature curve (figure 2). The required data were recorded on the dilatometer during the tests. The hollow specimens were inductively heated to 1100 °C in the dilatometer at different heating rates (1, 10, 100, 1000, 2000 and 2500 °Cs^{-1}). With the help of these tests involving different heating rates, the austenitisation process could be characterized in detail for different areas in the surface zone of the hot work tool steel to be investigated. To avoid oxidation, the tests were carried out under vacuum.

To characterize the austenitisation behaviour, the Ac_1 and Ac_3 temperatures at different constant heating rates were plotted to TTA diagram. Figure 3 shows the comparison of the Ac_1 and Ac_3 temperatures with respect to the heating rates for the materials under consideration. The two steels show similar austenitisation behaviour. An increase in Ac_1 and Ac_3 temperatures of up to 1000 °Cs^{-1} can be recorded. At heating rates greater than 1000 °Cs^{-1}, a drop in the Ac_1 and Ac_3 temperatures can be observed. The minimum Ac_1 temperatures are 803 °C for the 1.2367 and 814 °C for the 1.2343.

During a forging process, in addition to high thermal stresses, high mechanical tool stresses also occur in the die. These have a significant influence on the austenitization behaviour and can lead to a reduction of the Ac_1 temperature in hot work steels. To take this effect into account, the austenitization behaviour of both materials was additionally investigated by applying a mechanical load. In order to avoid plastic deformations in the subsequent austenitization tests under influence of mechanical load, the yield stress was determined at the minimum Ac_1 temperature. For this purpose, compression tests with cylinder samples (diameter = 5 mm and height = 10 mm) were used to record the yield curves of

the two materials (figure 4) and the corresponding load cases at yield stress (k_{f0}) were determined (table 2). A strain rate of 0.1 s^{-1} was considered for this purpose.

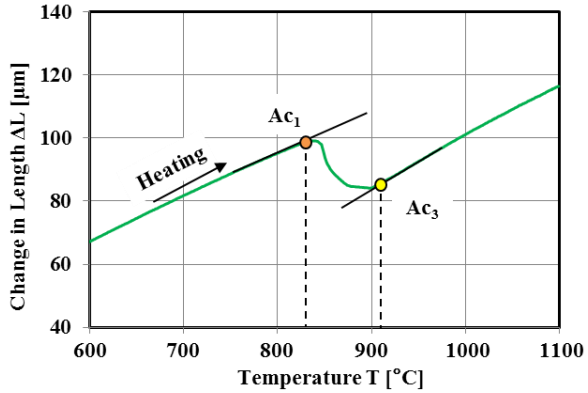

Figure 2. Determination of Ac_1 and Ac_3 temperatures by means of change in length (ΔL) – temperature (T) diagram.

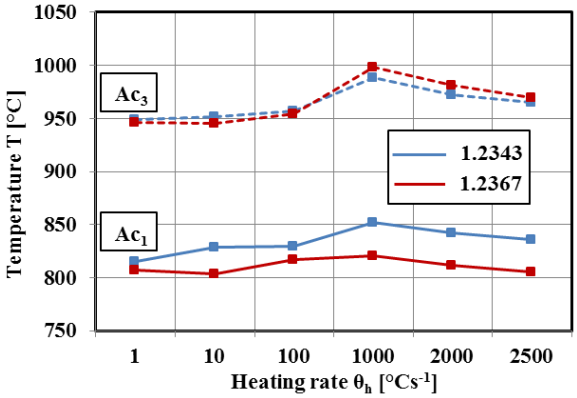

Figure 3. Comparison of Ac_1 and Ac_3 temperatures with respect to heating rates (θ_h) for tool steel 1.2343 and 1.2367.

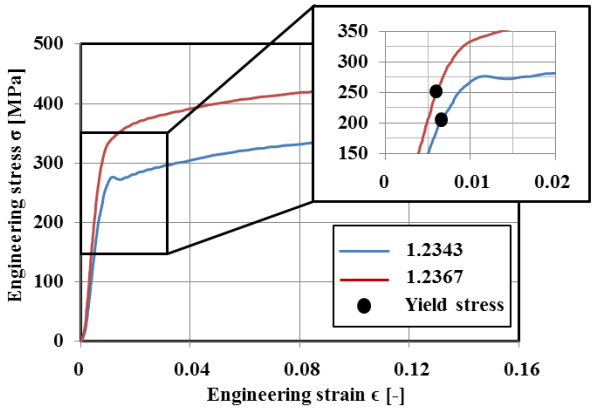

Figure 4. Evaluation of the yield stress from engineering stress-strain diagram for the tool steels 1.2343 and 1.2367.

Based on the calculated yield stress, the respective load cases to be tested (30 %, 50 % and 80 % of the k_{f0} stress) were defined for both materials (table 2). The force to be applied in the load superimposed tests was calculated corresponding to the specimen surface area (4.52 mm^2). The calculated mechanical loads were constantly applied to the hollow specimens during heating.

Table 2. Yield stress and evaluated load cases.

	k_{f0}	$F(k_{f0})$	$F(k_{f0}^{30\%})$	$F(k_{f0}^{50\%})$	$F(k_{f0}^{80\%})$
	MPa	N	N	N	N
1.2343	210	949	284	474	759
1.2367	250	1130	339	565	904

The results of the tests with superimposed loads are shown in figure 5 for both materials in relation to the different loads along with the initial results without influence of mechanical loads. It can be

observed that the Ac_1 temperature decreases with increasing load. The dependence on the heating rate corresponds to the previous tests without load superposition. The highest Ac_1 temperatures occur at 1000 °Cs^{-1} as before. At a heating rate of 1000 °Cs^{-1}, the Ac_1 temperature of material 1.2343 is reduced by 54 °C, 93 °C and 104 °C with respect to a load of 30 %, 50 % and 80 % of k_{f0} mechanical load as compared to the unloaded state (figure 5, left). For the material 1.2367, a reduction of the Ac_1 temperature by 14 °C, 26 °C and 44 °C can be observed at the heating rate of 1000 °Cs^{-1} for the material 1.2367, respectively for the load cases 30 %, 50 % and 80 % (figure 5, right). This shows that the mechanical load has a significant influence on the Ac_1 temperature and thus on the transformation behaviour of the tool steels. A lower Ac_1 temperature increases the probability of new hardening effects occurring, especially in areas subject to high mechanical stress.

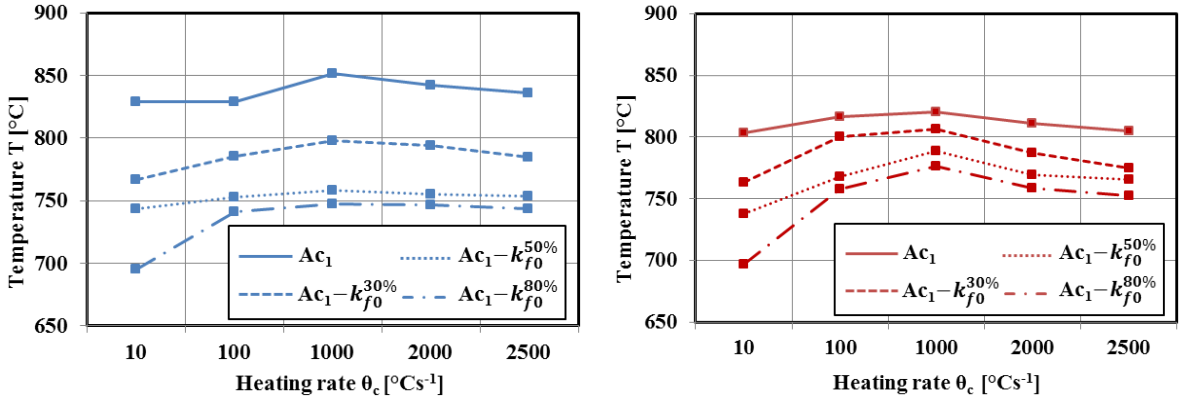

Figure 5. Effects of mechanical loads on the Ac_1 temperature for 1.2343 (left) and 1.2367 (right).

3.2. Continous-cooling-transformation (CCT) diagram

The continuous-cooling-transformation diagrams of the investigated materials are required to predict the mechanical properties that arise from different hardening conditions. The CCT tests were carried out using the quenching module of the deformation dilatometer and the results of experiments were evaluated according on the specifications of based on corresponding standards SEP 1680 and SEP 1681 [13, 14]. A constant heating rate of 1000 °Cs^{-1} was used to heat the hollow cylinder specimen till maximum temperature (T_{max} = 1100 °C) in vacuum conditions followed by a 10 seconds holding time at the maximum temperature. Subsequently, the heated specimens were quenched by using nine different cooling rates (0.1, 0.3, 0.5, 1, 5, 10, 25, 50 and 100 °Cs^{-1}). Nitrogen was used as a cooling medium for these tests. Following the experiments, the specimens were prepared for hardness measurements. For this purpose, the quenched hollow specimens were embedded in an epoxy resin. Micro-hardness measurements (HV0.2) were employed to evaluate the hardness of the embedded specimens using a 200 g test load with the Leica VMHT MOT hardness tester available at the IFUM. The temperature data obtained from experimental results were plotted against logarithmic time for all of the considered cooling rates mentioned above to obtain the CCT diagram (figure 6) of both the tool steels 1.2343 and 1.2367. The corresponding Vickers hardness values are also listed in the figure.

Based on experimental findings, it has been observed that both the steels have relatively low critical cooling rates ($\theta_{c,crit}$) of about 1 °Cs^{-1} due to their high carbon content. Cooling the steels at cooling rates higher than the critical cooling rate resulted in a significant increase in hardness of the specimen, namely hardness values greater than 800 HV0.2. Whereas, the lower cooling rates (0.1, 0.3 and 0.5 °Cs^{-1}) led to increase in bainite content in the microstructure. The formation of pearlitic (P), bainitic (B) and martensitic (M) and carbidic (C) phase fractions from the initial austenitic (A) phase was observed (figure 6, left) for the tool steel 1.2343. On the contrary, pearlitic phase was not observed for the tool steel 1.2367 (figure 6, right). Moreover, the high carbide percentage existing due to increased chromium content in both the steels prevents formation of bainite and instead majority of the austenite grains are transformed into martensite at cooling rates higher than the critical cooling rates. The minimum

martensitic start (M_s) and end (M_f) temperatures were observed as 280 °C and 125 °C respectively for both the tool steels.

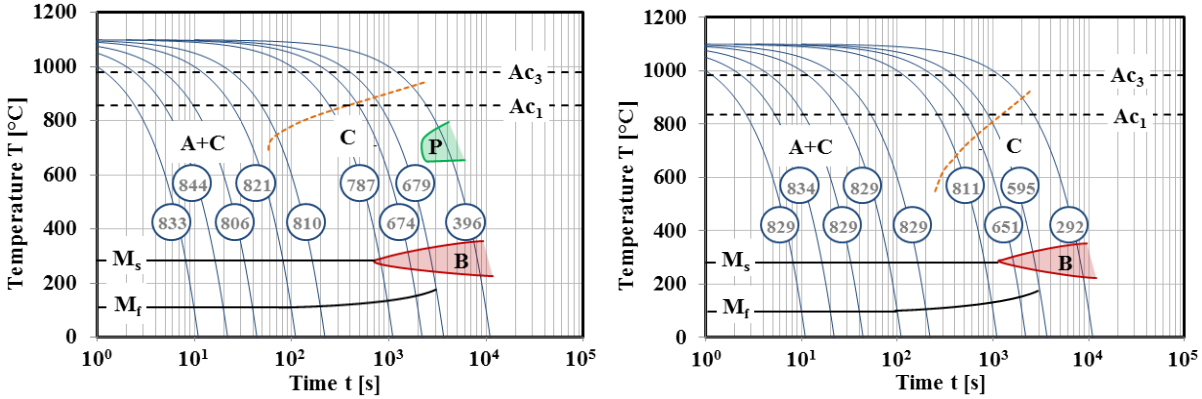

Figure 6. Continuous-time-temperature diagram for both the tool steels, 1.2343 (left) and 1.2367 (right).

Metallographic tests were performed on the specimens from experimental CCT experiments and a purely martensitic microstructure was observed for all specimens cooled with critical cooling rates or higher. The microstructure images of specimen for tests performed at the critical cooling rate are exemplarily shown in figure 7.

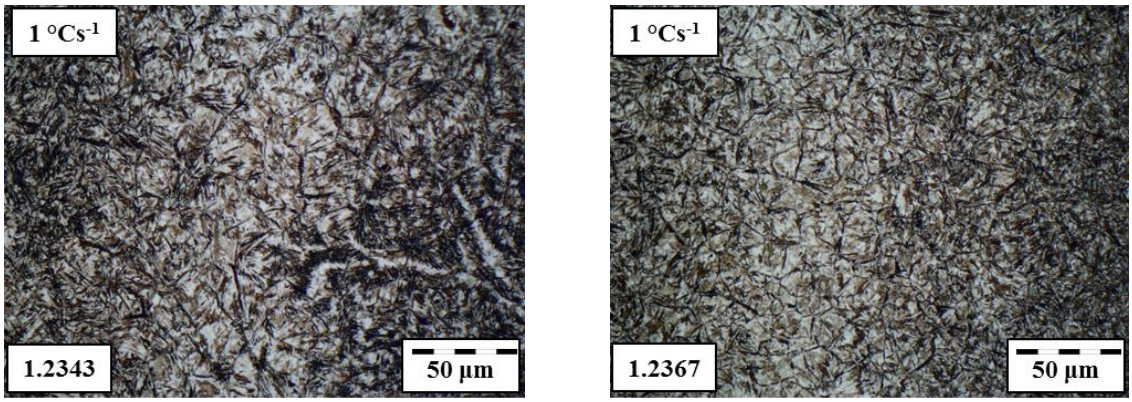

Figure 7. Specimen microstructure for tests at critical cooling rate ($\theta_{c,crit}$), 1.2343 (left) and 1.2367 (right).

4. Conclusion

Tools in hot forging experience cyclic high heating and subsequent cooling which can lead to local changes in the tool microstructure and hence a hardening or softening of the material in various tool regions consequently influencing the tool strength. Besides, high thermo-mechanical loadings acting on the tools during such processes result in temperatures exceeding the austenitic temperatures locally. In the scope of this paper, the austenitisation behaviours of two hot-work tool steels, 1.2343 and 1.2367, have been characterized by means of time-temperature-austenitization (TTA) diagrams for specimens under thermo-mechanical loads. It was observed that the application of mechanical loads, along with thermal loads, leads to lowering of the Ac_1 temperature. Moreover, continuous cooling transformation (CCT) diagrams were recorded to examine the phase transformation and hardness behaviour in the tested specimens. A fully martensitic transformation was observed for both the materials at all the cooling rates above 1 °Cs^{-1}. In future work, these findings will be used to design the temperature profiles for cyclic thermo-mechanical tests and subsequently tool hardness profiles in relation with the number of process cycles, mechanical loads and the process temperature will be evaluated in order to develop an improved wear methodology.

Acknowledgements
Results presented here are from the research project "New hardening and tempering effects II" (grant number IGF 19647N). This project has been funded by the German Federal Ministry of Economics and Energy via the German Federation of Industrial Cooperative Research Associations "Otto von Guericke" (AiF) in the program to encourage the industrial Community research by a resolution of the German Bundestag and the Steel Forming Research Society (FSV).

References
[1] Kannappan A 1969 Wear in Forging Dies – A Review of World Experiences *Metal Forming* **36** 335-43
[2] Summerville E, Venkatesan K and Subramanian C 1995 Wear processes in hot forging press tools, *Materials & Design* **16** 289-94
[3] Bartz J W and Barnert L 2004 Handbook of Tribology and Lubrication *Tribology and Lubrication in Massive Forming* (Expert-Verlag Renningen) **13** Chapter 6 140-86
[4] Saiki H, Marumo Y, Minami A and Sonoi T 2001 Effect of the surface structure on the resistance to plastic deformation of a hot forging tool *J. Mat. Proc. Tech.* **113** 22-7
[5] Behrens B-A, Bouguecha A, Vucetic M and Chugreev A 2016 Advanced Wear Simulation for Bulk Metal Forming Processes *MATEC Web Conf.* **80** 04003
[6] Dean T A and Silva T M 1979 Die temperatures during production drop forging *ASME J. Eng. Ind.* **101** 385-90
[7] Jeong D J, Kim D J, Kim J H, Kim B M and Dean T A 2001 Effects of surface treatments and lubricants for warm forging die life *J. Mat. Proc. Tech.* **113** 544-50
[8] Behrens B-A, Bouguecha A, Bonk C and Chugreev A 2017 Numerical and experimental investigations of the anisotropic transformation strains during martensitic transformation in a low alloy Cr-Mo steel 42CrMo4 *Procedia Engineering* **207** 1815-20
[9] Behrens B-A, Bouguecha A, Bonk C and Chugreev A 2017 Experimental investigations on the transformation-induced plasticity in a high tensile steel under varying thermo-mechanical loading *Computer Methods in Materials Science* **17** 36-43
[10] Wever F, Rose A, and Peter W 1961 *Atlas zur Wärmebehandlung der Stähle* **1&2** (Düsseldorf: Verlag Stahleisen).
[11] Orlich J, Rose A, and Wiest P 1973 *Atlas zur Wärmebehandlung der Stähle* **3** (Düsseldorf: Verlag Stahleisen).
[12] Behrens B-A, Chugreev A and Kock C 2018 Experimental-numerical approach to efficient TTT-generation for simulation of phase transformations in thermomechanical forming processes *IOP Conf. Ser. Mater. Sci. Eng.* **461** 012040
[13] SEP 1680 1990 STAHL-EISEN-Prüfblätter (SEP) 3rd Ed.
[14] SEP 1681 1998 STAHL-EISEN-Prüfblätter (SEP) 2nd Ed.